

**Polymeric monolithic microcartridges with gold nanoparticles for the analysis of protein biomarkers by on-line solid-phase extraction capillary electrophoresis-mass spectrometry**

Laura Pont<sup>1</sup>, Gemma Marin<sup>1</sup>, María Vergara-Barberán<sup>2</sup>, Leonardo G. Gagliardi<sup>3</sup>,  
Victoria Sanz-Nebot<sup>1</sup>, José M. Herrero-Martínez\*<sup>2</sup>, Fernando Benavente\*<sup>1</sup>

<sup>1</sup>Department of Chemical Engineering and Analytical Chemistry, Institute for Research on Nutrition and Food Safety (INSA·UB), University of Barcelona, C/Martí i Franquès 1-11, 08028 Barcelona, Spain

<sup>2</sup>Department of Analytical Chemistry, University of Valencia, C/Doctor Moliner 50, 46100 Burjassot, Spain

<sup>3</sup>Laboratorio de Investigación y Desarrollo de Métodos Analíticos, LIDMA, Facultad de Ciencias Exactas, Universidad Nacional de La Plata, CIC-PBA CONICET, C/ 47 esq. 115, B1900AJL La Plata, Argentina

\*Corresponding authors: fbenavente@ub.edu (F. Benavente, PhD)

Tel: (+34) 934039116, Fax: (+34) 934021233

and jmherrer@uv.es (J. M. Herrero-Martínez, PhD)

Tel: (+34) 963544062, Fax: (+34) 963544436

**KEYWORDS:** capillary electrophoresis / gold nanoparticles / mass spectrometry / monolithic microcartridge / on-line solid-phase extraction / transthyretin

1 **ABSTRACT**

2 In this study, polymeric monoliths with gold nanoparticles (AuNP@monolith) were  
3 investigated as microcartridges for the analysis of protein biomarkers by on-line solid-  
4 phase extraction capillary electrophoresis-mass spectrometry (SPE-CE-MS). “*Plug-and-*  
5 *play*” microcartridges (7 mm) were prepared from a glycidyl methacrylate (GMA)-  
6 based monolithic capillary column (5 cm x 250  $\mu\text{m}$  i.d.), which was modified with  
7 ammonia and subsequently functionalized with gold nanoparticles (AuNPs). The  
8 performance of these novel microcartridges was evaluated with human transthyretin  
9 (TTR), which is a protein related to different types of familial amyloidotic  
10 polyneuropathies (FAP). Protein retention depended on the isoelectric point of the  
11 protein (TTR pI~5.4) and elution was achieved with a basic phosphate solution. Under  
12 the optimized conditions, limits of detection (LODs) for TTR by AuNP@monolith-  
13 SPE-CE-MS were 50 times lower than by CE-MS (5 vs 250  $\text{mg}\cdot\text{L}^{-1}$ , with an ion trap  
14 (IT) mass spectrometer). The sensitivity enhancement was similar compared to SPE-  
15 CE-MS using immunoaffinity (IA) microcartridges with intact antibodies against TTR.  
16 Linearity, repeatability in migration times and peak areas, reusability, reproducibility  
17 and application to serum samples were also evaluated.

18

19

## 20 **1. Introduction**

21 One of the issues that affects the limits of detection (LODs) of high-performance  
22 separation techniques at the microscale is the reduced volume of sample that must be  
23 analyzed to obtain optimum separations [1–6]. This is the case of capillary  
24 electrophoresis-mass spectrometry (CE-MS) that has been combined with different  
25 electrophoretic and chromatographic strategies to enhance sensitivity [1–6], such as  
26 those based on on-line solid-phase extraction (SPE) [4–6]. Today, the on-line coupling  
27 of SPE to CE-MS (SPE-CE-MS) is widely accepted as a highly versatile and efficient  
28 sensitivity enhancement approach [5,6]. The typical SPE-CE-MS configuration without  
29 valves is very simple [6], with the microcartridge connected in series close to the inlet  
30 of the separation capillary. The sorbent contained in the microcartridge allows retaining  
31 the target analyte from a large sample volume. Then, the retained analyte is  
32 subsequently cleaned-up and preconcentrated in a smaller volume of eluent before the  
33 electrophoretic separation and MS detection.

34

35 The main limitation to broad the applicability of SPE-CE-MS is that the modified  
36 capillaries must be lab-made because they are not commercially available [6]. The most  
37 widely used microcartridges are packed with sorbent particles, which are typically  
38 retained between one or two frits to avoid particle leaking during the analyses [7].  
39 Nevertheless, frits may promote column back-pressure, electroosmotic flow (EOF)  
40 disturbance, bubble formation and current instability or breakdowns. Fritless particle-  
41 packed microcartridges have been also described, by simply using to prevent bleeding,  
42 magnetic particles or sorbents with particle size slightly greater than the inner diameter  
43 of the separation capillary [6]. However, the construction of particle-packed  
44 microcartridges continues to be perceived as challenging for non-experienced users, and

45 several other alternatives have been proposed based on sorbent membranes, fibers,  
46 coatings or monoliths [6].

47

48 Fritless monolithic microcartridges are probably the best choice to simplify and  
49 systematize the reproducible construction of particle-free microcartridges [8–17]. A  
50 monolithic sorbent is a continuous unitary porous structure without inter-particle voids  
51 that can be synthesized inside the separation capillary (“in situ”) [8–12] or as a capillary  
52 column of a certain length (“ex situ”) to cut later several “plug-and-play”  
53 microcartridges [13–17]. At best, the monolithic sorbent fills completely the  
54 microcartridge lumen [8–16]. Furthermore, the monolith physical structure (*e.g.*  
55 porosity and pore size) and the number and type of active surface groups can be further  
56 tailored to maximize extraction selectivity and recovery without compromising fluidic  
57 and electric performance in SPE-CE. In this sense, the use of gold nanoparticles  
58 (AuNPs) in combination with polymeric monoliths (AuNP@monolith) has been  
59 explored in separation and sample pretreatment due to their high-surface-area-to-  
60 volume ratios, easy chemical modification and strong affinity for thiol-containing  
61 compounds [18–23]. Indeed, the application of AuNP@monoliths for the analysis of  
62 cysteine-containing peptides, proteins and other compounds [18–23] or as a platform to  
63 facilitate further variations in surface functionalities [19,24–27] has been reported.  
64 However, despite the greater potential of these hybrid monoliths compared to other  
65 monolithic sorbents from the point of view of ease of preparation, high extraction  
66 capacity and versatility of functionalization, their integration as microcartridges for  
67 SPE-CE-MS has not been explored yet

68

69 In this study, polymeric AuNP@monoliths were investigated for the first time as  
70 microcartridges in SPE-CE-MS. For this purpose, “plug-and-play” microcartridges were  
71 prepared from a glycidyl methacrylate (GMA)-based monolithic capillary column,  
72 which was modified with ammonia and subsequently functionalized with AuNPs  
73 [22,23]. The performance of the microcartridges was evaluated with human  
74 transthyretin (TTR), which is a protein related to different types of familial amyloidotic  
75 polyneuropathies (FAP) [28–30]. Protein loading and elution conditions were optimized  
76 to obtain the best protein recoveries and the method was validated using an ion trap (IT)  
77 mass spectrometer in terms of linearity, limits of detection (LODs), repeatability in  
78 migration times and peak areas, microcartridge lifetime and reproducibility. The  
79 sensitivity enhancement by AuNP@monolith-SPE-CE-MS was discussed compared to  
80 CE-MS and immunoaffinity SPE-CE-MS (IA-SPE-CE-MS). The method was further  
81 demonstrated using an accurate mass and high-resolution time-of-flight (TOF) mass  
82 spectrometer before the analysis of serum samples.

83

## 84 **2. Experimental section**

### 85 **2.1. Materials and reagents**

86 All the chemicals used in the preparation of background electrolytes (BGEs) and  
87 solutions were of analytical reagent grade or better. 3-(trimethoxysilyl) propyl  
88 methacrylate (98%), glycidyl methacrylate (GMA,  $\geq 97\%$ ), ethylene glycol  
89 dimethacrylate (EDMA,  $\geq 98\%$ ) and azobisisobutyronitrile (AIBN, 98%) were  
90 purchased from Sigma-Aldrich (Steinheim, Germany). Acetic acid (HAc) (glacial),  
91 ammonium hydroxide (25%), formic acid (HFor) (99.0%), potassium  
92 dihydrogenphosphate ( $\geq 99.0\%$ ), sodium hydrogenphosphate ( $\geq 99.0\%$ ), ammonium  
93 dihydrogenphosphate ( $\geq 99.0\%$ ), phenol ( $\geq 99.5\%$ ), and human transthyretin (TTR)

94 ( $\geq 95.0\%$ ) were acquired from Merck (Darmstadt, Germany). Acetonitrile (LC-MS),  
95 methanol (99.9% (v/v)) and ethanol (96% (v/v)) were supplied by Panreac AppliChem  
96 (Barcelona, Spain). Ammonium acetate ( $\text{NH}_4\text{Ac}$ ) ( $\geq 99.9\%$ ) and Tween<sup>®</sup> 20 were  
97 provided by Sigma-Aldrich. Propan-2-ol (LC-MS) and AuNP dispersion (particle size,  
98 20 nm, stabilized with sodium citrate) were supplied by Fluka (Buchs, Switzerland) and  
99 Alfa Aesar (Lancashire, United Kingdom), respectively. LC-MS grade water (Fisher  
100 Scientific, Loughborough, UK) was used in experiments involving MS detection. For  
101 the rest of experiments, water with a conductivity value lower than  $0.05 \mu\text{S}\cdot\text{cm}^{-1}$  was  
102 obtained using a Milli-Q water purification system (Millipore, Molsheim, France).  
103 Fused silica capillaries were supplied by Polymicro Technologies (Phoenix, AZ, USA).

104

## 105 **2.2. Electrolyte solutions, sheath liquid, protein standard and blood sample**

106 All solutions were degassed for 10 min by sonication and filtered through a  $0.20 \mu\text{m}$   
107 nylon filter (MSI, Westboro, MA, USA) before use. The BGEs for the CE-MS and  
108 AuNP@monolith-SPE-CE-MS studies contained 1 M HAc (pH 2.3) (acidic BGE) or 10  
109 mM  $\text{NH}_4\text{Ac}$ , pH 5.0 (pI BGE). The sheath liquid solution was a mixture of 60:40 (v/v)  
110 propan-2-ol/water with 0.05% (v/v) or 0.25 % (v/v) of HFor for the acidic or the pI  
111 BGEs, respectively.

112 An aqueous standard solution ( $1,000 \mu\text{g}\cdot\text{mL}^{-1}$ ) of TTR was prepared and stored  
113 in a freezer at  $-20^\circ\text{C}$  until its use. Excipients of low molecular mass were removed by  
114 passage through 10,000 relative molecular mass ( $M_r$ ) cut-off cellulose acetate filters  
115 (Amicon Ultra-0.5, Millipore) [28]. The sample was centrifuged at  $25^\circ\text{C}$  for (10 min at  
116  $11,000 \times g$ ) and the residue was washed three times with an appropriate volume of  
117 water or BGE in the same way. The final residue was recovered by inverting the upper  
118 reservoir in a vial and spinning once more at a reduced centrifugal force (2 min at  $300 \times$

119 g). Enough water or BGE were added to adjust the concentration of TTR to 1,000  
120  $\mu\text{g}\cdot\text{mL}^{-1}$ .

121 Fresh blood from a healthy donor (male, 43-years old) was obtained by  
122 venepuncture and serum was prepared as described in our previous work [28]. The  
123 assay was approved by the Ethics Committee of the UB and written informed consent  
124 was obtained from the donor. Serum aliquots were stored in a freezer at  $-20^{\circ}\text{C}$  when not  
125 in use.

126

### 127 **2.3. Apparatus**

128 pH measurements were made with a Crison 2002 potentiometer and a Crison  
129 electrode 52-03 (Crison Instruments, Barcelona, Spain). Agitation was performed with a  
130 Vortex Genius 3 (Ika<sup>®</sup>, Staufen, Germany). Centrifugal filtration was carried out in a  
131 cooled Rotanta 460 centrifuge (Hettich Zentrifugen, Tuttlingen, Germany).

132 A KD Scientific 100 series infusion pump (Holliston, MA, USA) was used to  
133 modify the GMA-based monolithic capillary column with ammonia and AuNPs, as well  
134 as for delivery of the sheath liquid in CE-MS and AuNP@monolith-SPE-CE-MS  
135 experiments.

136

### 137 **2.4. CE-MS**

138 All CE-MS experiments were performed in a 7100 CE coupled with an  
139 orthogonal G1603A sheath-flow interface to a LC/MSD Ion Trap (IT) SL or a 6220 oa-  
140 Time-of-flight (TOF) LC/MS mass spectrometer (Agilent Technologies, Waldbronn,  
141 Germany). LCMSD Trap software (Bruker Daltonik, Bremen, Germany) or  
142 ChemStation and MassHunter softwares (Agilent Technologies) were used for the CE-  
143 IT-MS and CE-TOF-MS instrument control, data acquisition and processing,

144 respectively. The mass spectrometers were operated in ESI+ mode as described in some  
145 of our previous works [28–31]. With the IT mass spectrometer, full scan mass spectra  
146 were acquired from 700 to 2,200 m/z. ESI, capillary exit, skimmer, octopole 1, octopole  
147 2, octopole radiofrequency, lens 1 and lens 2 voltages were set at 4000 V, 260 V, 30 V,  
148 3.0 V, 2.5 V, 225 V, -2.8 V and -80 V respectively, with the trap drive at 95 (arbitrary  
149 units) [31]. With the TOF mass spectrometer, full scan mass spectra were acquired from  
150 100 to 3,200 m/z in the high-resolution mode (4 GHz). Capillary, fragmentor, skimmer  
151 and OCT 1 RF voltages were set at 4,000 V, 325 V, 80 V and 300 V, respectively [28–  
152 30]. In both mass spectrometers, nebulizer gas (N<sub>2</sub>) pressure was 7 psi, drying gas (N<sub>2</sub>)  
153 flow rate was 4 L·min<sup>-1</sup> and drying gas temperature was set at 300°C. The sheath liquid  
154 was delivered at a flow rate of 3.3 μL·min<sup>-1</sup> [28–31].

155

156 CE-MS separations were performed at 25°C in a 72 cm total length ( $L_T$ ) × 75  
157 μm internal diameter (i.d.) × 365 μm outer diameter (o.d.) capillary [28,29]. All  
158 capillary rinses were performed flushing at 930 mbar. For new capillaries or between  
159 workdays, the capillary was activated flushing with 1 M NaOH (20 or 5 min,  
160 respectively), water (20 or 5 min), and BGE (20 or 10 min) (both procedures were  
161 performed off-line to avoid the unnecessary contamination of the MS system). Between  
162 analyses the capillary was conditioned flushing with water (2 min) and BGE (2 min).  
163 Samples were hydrodynamically injected at 50 mbar for 10 s (54 nL, i.e. 1.7% of the  
164 capillary, estimated using the Hagen–Poiseuille equation [32]), and a separation voltage  
165 of +25 kV (normal polarity, cathode in the outlet) was applied. With the pI BGE (pH  
166 5.0), 100 mbar of pressure were also applied during the electrophoretic separation. The  
167 autosampler was kept at 10°C using an external water bath (Minichiller 300, Peter

168 Huber Kältemaschinenbau AG, Offenburg, Germany). For short or overnight storage,  
169 the capillary was flushed with water (2 min).

170

#### 171 **2.4. Preparation of AuNP@monolith microcartridges for SPE-CE-MS**

172 The GMA-*co*-EDMA monolith was prepared as described in a previous work  
173 [22]. Briefly, the polymerization mixture was prepared in a 10 mL glass vial by  
174 weighing the monomers GMA (20% (m/m)) and EDMA (5% (m/m)), and a binary  
175 porogenic solvent mixture of cyclohexanol (70 % (m/m)) and 1-dodecanol (5% (m/m)).  
176 AIBN was added as initiator (1% (m/m) with respect to the monomers). The final  
177 mixture was sonicated for 5 min and then purged 10 min with nitrogen to remove  
178 oxygen.

179 In order to ensure the covalent attachment of the polymer monolith, the inner  
180 wall of a fused silica capillary (1 m  $L_T$  x 250  $\mu\text{m}$  i.d. x 365  $\mu\text{m}$  o.d.) was modified with  
181 3-(trimethoxysilyl)propyl methacrylate as described elsewhere [33]. Then, a 5 cm  
182 fragment of the silanized capillary was cut and the polymerization mixture was  
183 introduced slowly by hand to avoid bubble formation, using a plastic syringe with an  
184 appropriate connector. The capillary column was sealed at both ends with two rubber  
185 septa and it was polymerized in an oven at 60 °C for 24 h. After the polymerization  
186 reaction was completed, the generic polymer was washed with methanol (30 min) to  
187 remove the porogenic solvents and the unreacted monomers. Next, a 4.5 M ammonium  
188 hydroxide solution was pumped through the GMA-based monolith at 60°C (using a  
189 column oven) at a flow rate of 100  $\mu\text{L}\cdot\text{h}^{-1}$  for 2 h. The capillary column was then  
190 flushed with water at room temperature until neutral pH. Afterwards, citrate-stabilized  
191 AuNPs colloidal dispersion was pumped through the monolithic capillary at room  
192 temperature at a flow rate of 200  $\mu\text{L}\cdot\text{h}^{-1}$ , until the entire monolith length turned deep red

193 and a pink solution was observed coming out from the capillary outlet. Finally, the  
194 column was thoroughly washed with water (30 min). The surface coverage of monolith  
195 with AuNPs was also confirmed by SEM (see Fig. S1A), and its Au content was  
196 estimated to be *ca.* 14 % m/m by energy dispersive X-ray (EDAX) (see Fig. S1B).

197 The AuNP@monolith capillary column was cleanly cut into 7 mm pieces to  
198 prepare the fritless monolithic microcartridges. The microcartridge was connected using  
199 two plastic sleeves at 7.5 cm from the inlet of a 72 cm  $L_T \times 75 \mu\text{m i.d.} \times 365 \mu\text{m o.d.}$   
200 capillary, which was previously activated as in CE-MS. The junction was tight enough  
201 to avoid adhesive sealing, hence the microcartridge was “plug-and-play” and  
202 completely replaceable. A plastic syringe with an appropriate connector was used to  
203 check the system for abnormal flow restriction, taking as a reference the flow through a  
204 CE-MS capillary of the same dimensions.

205 For AuNP@monolith-SPE-CE-MS under the optimized conditions, the capillary  
206 with the microcartridge was first conditioned flushing at 930 mbar with water (2 min)  
207 and BGE (2 min). Next, sample dissolved in the pI BGE (pH 5.0) was introduced at 930  
208 mbar for 5 min (30  $\mu\text{L}$  [32]). Then, a flush with pI BGE (1 min) allowed removing non  
209 retained molecules and filling the capillary before the elution. All these steps were  
210 performed with the nebulizer gas and the ESI capillary voltage switched off to prevent  
211 the entrance of contaminants into the MS. Then, both were switched on and a small  
212 volume of eluent was injected at 50 mbar for 20 s (108 nL [32], 30 mM  $(\text{NH}_4)_2\text{H}_2\text{PO}_4$   
213 adjusted to pH 9.0 with ammonium hydroxide). The separation was conducted applying  
214 +25 kV and assisting with 100 mbar. Between consecutive runs, to avoid carry-over, the  
215 capillary was flushed with eluent (1 min) and water (1 min). Separations were  
216 performed at 25°C with the autosampler at 10°C. The rest of experimental conditions  
217 were as in CE-MS.

## 218 **2.5 Quality parameters**

219 TTR migration times and peak areas were obtained from the extracted ion  
220 electropherograms (EIEs) of the most abundantly detected molecular ions (i.e. +7 and  
221 +8 molecular ions of monomeric (MO) TTR with the IT mass spectrometer). In  
222 AuNP@monolith-SPE-CE-MS, repeatability (n=3) was evaluated as the relative  
223 standard deviation (%RSD) of migration times and peak areas for a 10  $\mu\text{g}\cdot\text{mL}^{-1}$  TTR  
224 standard. Linearity range was studied in the concentration range between 5 and 50  $\mu\text{g}$   
225  $\text{mL}^{-1}$ . LODs were estimated by analyzing low-concentration TTR standards (close to  
226 the LOD level, as determined from the approach based on  $S/N=3$ ). The microcartridge  
227 lifetime was evaluated by repeatedly analyzing a 10  $\mu\text{g}\cdot\text{mL}^{-1}$  TTR standard.

228

## 229 **2.6 Analysis of serum samples**

230 Serum samples were pretreated off-line before the analysis of TTR to deplete other  
231 high-abundance proteins. This should prevent microcartridge saturation and protein  
232 adsorption on the capillary inner surface. The applied off-line sample pretreatment  
233 method performed good for the analysis of TTR by IA-SPE-CE-MS [30]. Eight mg of  
234 NaCl were added at 2°C to 100  $\mu\text{L}$  of human serum followed by 100  $\mu\text{L}$  of 5% (v/v)  
235 phenol dropwise to precipitate the proteins. The supernatant was collected after  
236 centrifugation at 25 °C (10 min at 11,000 x g) and then diluted 1:1 (v/v) with the pI  
237 BGE (pH 5.0) before its analysis by SPE-CE-MS.

238

## 239 **3. Results and discussion**

### 240 **3.1. CE-MS**

241 In a previous investigation, a CE-TOF-MS method was developed for the  
242 analysis of TTR using an acidic BGE with 1 M HAc (pH 2.3) and a sheath liquid with

243 60:40 (v/v) propan-2-ol/water with 0.05% (v/v) of HF<sub>or</sub> [28,29]. The acidic BGE  
244 allowed the best sensitivity for the analysis of TTR because of the higher ionization  
245 efficiency of proteins in positive ESI mode at very low pH values. In this particular  
246 case, the acidic BGE also promoted disruption of the native tetrameric structure of TTR,  
247 hence monomeric (MO) TTR proteoforms were only detected. The same method was  
248 applied here using a conventional IT mass spectrometer. This mass spectrometer is not  
249 the most ideal choice to analyze proteins due to the limited mass accuracy, mass  
250 resolution, scanning speed and m/z scanning ranges. However, it performs reasonably  
251 well to obtain average molecular mass values of proteins of considerable complexity,  
252 such as we have demonstrated for transferrin or recombinant human erythropoietin [31].  
253 Therefore, it is very convenient for method optimization in CE-MS and SPE-CE-MS  
254 without resorting to a more appropriate, but less available, mass spectrometer (e.g. an  
255 accurate mass high-resolution TOF mass spectrometer). Figures 1A and 1B (parts i))  
256 show the total ion electropherogram (TIE) and the mass spectrum obtained by CE-IT-  
257 MS for a 500  $\mu\text{g}\cdot\text{mL}^{-1}$  standard solution of TTR using the acidic BGE (pH 2.3),  
258 respectively. TTR appears in the electropherogram as a sharp single peak, and the mass  
259 spectrum shows the typical cluster of multiply charged ions of MO TTR (with m/z of  
260 the most abundant molecular ion corresponding to the MO with charge +9). Indeed, as  
261 hinted before, the performance of the IT mass spectrometer was not enough to obtain  
262 information about the different MO TTR proteoforms, but only an average  $M_r$  for the  
263 target protein (i.e.  $M_{r \text{ exp}} = 13,880$ ) which is close to the most abundant MO TTR  
264 proteoform (i.e. TTR showing a mixed disulfide with the amino acid cysteine at position  
265 10 of the sequence, TTR-Cys,  $M_{r \text{ theo}} = 13,880.4022$ ) [28,29].

266 As an alternative to the acidic BGE (pH 2.3), a BGE with 10 mM NH<sub>4</sub>Ac, pH  
267 5.0 (pI BGE) was also investigated to analyze TTR by CE-IT-MS. At this pH value,

268 TTR was close to its pI (5.4), and its retention onto the AuNP surface was expected to  
269 be maximum, as indicated before. This is what we observed when a similar  
270 methacrylate monolith modified with AuNPs was ground and used as a sorbent for the  
271 isolation of bovine serum albumin, cytochrome c and mistletoe leave lectins by off-line  
272 SPE [22]. Figures 1A and B (parts ii)) show the TIE and the mass spectrum obtained for  
273 a  $500 \mu\text{g}\cdot\text{mL}^{-1}$  standard solution of TTR using the pI BGE (pH 5.0), respectively. As  
274 can be observed in Figure 1A ii), TTR was now detected at a shorter migration time.  
275 The cathodic EOF at pH 5.0 was higher than at pH 2.3, but this was mainly due to the  
276 application of 100 mbar of pressure during the electrophoretic separation at 25 kV.  
277 Without applying a positive pressure between 25 and 100 mbar, analyses were  
278 precluded due to the frequent current interruptions and the poor reproducibility. Since  
279 total analysis time was shorter by applying 100 mbar, this pressure was selected for  
280 further analyses. Furthermore, in order to achieve an appropriate sensitivity (30%  
281 increase of TTR peak intensity), it was necessary to increase the HFor content in the  
282 60:40 (v/v) propan-2-ol/water sheath liquid until 0.25 % (v/v). Under these conditions,  
283 the mass spectrum of TTR (Figure 1B ii)) shows that the cluster of multiply charged  
284 ions of MO TTR was shifted to higher m/z values (with m/z of the most abundant  
285 molecular ion corresponding to the MO with charge +8). Besides, as expected,  
286 sensitivity was better with the BGE of lower pH (see the TTR peak intensity in both  
287 TIEs of Figure 1A for comparison), hence LODs for TTR were 50 and  $250 \mu\text{g}\cdot\text{mL}^{-1}$ ,  
288 respectively. Repeatability of migration time and peak area with the pI BGE (pH 5.0)  
289 was good (i.e. 2.3% and 6.0%, n=3, respectively) and similar to the values with the  
290 acidic BGE (pH 2.3) (i.e. 3.4% and 4.8%, n=3, respectively).

291

### 292 **3.2 AuNP@monolith-SPE-CE-MS**

293 Protein adsorption onto AuNP surfaces is a complex phenomenon, which is  
294 mainly driven by electrostatic and hydrophobic interactions. Electrostatic interactions  
295 can be explained by the presence of the positively charged basic groups of the proteins  
296 and the negatively charged citrate-stabilized AuNPs. Hydrophobic interactions are  
297 mainly due to the free amino, imidazole and thiol groups in the side chains of the amino  
298 acid residues, which displace citrate from the Au surface [34–36]. Different studies have  
299 shown that Au surfaces can effectively retain proteins within an appropriate pH range.  
300 In a previous investigation [22], we observed that protein retention was specially  
301 favored at a pH close to the protein pI, where the hydrophobic interactions are supposed  
302 to be predominant.

303 Despite these considerations, and taking into account the CE-MS results showed  
304 in the previous section, we decided to perform the first SPE-CE-MS experiments using  
305 the acidic BGE (pH 2.3) for the separation and loading TTR standard solutions in water  
306 or in the pI BGE (pH 5.0). However, results were not satisfactory, and no protein was  
307 detected. This was probably due to elution of TTR during the washing step with the  
308 acidic BGE (pH 2.3). The washing step allows removing impurities and poorly retained  
309 TTR after sample loading and it is mandatory to fill the capillary before the elution,  
310 separation and detection. In order to improve protein recoveries, different BGEs with 10  
311 mM NH<sub>4</sub>Ac and pH values close to the TTR pI were investigated (i.e. pH 4.2, 5.0 and  
312 5.8). In all cases, TTR standard solutions were loaded in the corresponding BGE, as no  
313 TTR was detected when the protein was loaded in water. Elution was performed at basic  
314 pH, in accordance to our experience with the ground methacrylate monolith modified  
315 with AuNPs [22]. However, the solution providing the best results in that study (20 mM  
316 sodium phosphate, pH 12.0) was avoided, because it is well-known that the presence of  
317 sodium cations and phosphate anions decreases ionization efficiency in MS. As an

318 alternative, based on our previous research with immobilized metal affinity SPE-CE-  
319 MS [37], a small plug (i.e. 20s at 50 mbar) of 30 mM (NH<sub>4</sub>)H<sub>2</sub>PO<sub>4</sub>, pH 9.0 was used.  
320 Figure 2 shows the TIEs obtained for a 20 µg·mL<sup>-1</sup> standard solution of TTR using each  
321 BGE and these elution conditions. As can be observed, the most intense TTR peak was  
322 detected at pH 5.0 (i.e. pI BGE), hence this BGE was selected for the rest of  
323 experiments. At these conditions, TTR was detected as a single peak (Figure 2B), as in  
324 CE-MS (Figure 1A ii)). However, the peak was slightly broader and migration time  
325 longer, due to the combined effect of the differences on pH and composition of the  
326 eluent and the pI BGE and the backpressure promoted by the microcartridge. With  
327 regard to the sample loading, the sample loading time was studied by introducing a 20  
328 µg·mL<sup>-1</sup> standard solution of TTR at 930 mbar from 2 to 20 min. As can be seen in  
329 Figure 3A, the maximum amount of TTR was detected with a 5 min loading time (30  
330 µL of sample, see Section 2.4). When the protein solution was loaded for a longer time,  
331 analyte breakthrough caused a significant decrease of peak area. Consequently, in order  
332 to reduce the total analysis time while achieving the highest recoveries, a sample  
333 loading time of 5 min was selected for the rest of experiments.

334         Once selected the pI BGE (pH 5.0) for sample loading, washing and separation  
335 and the sample loading time, different volatile eluents covering acidic and basic pH  
336 values were tested as an alternative to the 30 mM (NH<sub>4</sub>)H<sub>2</sub>PO<sub>4</sub>, pH 9.0 solution.  
337 However, acidic eluents (i.e. 1 M HAc, pH 2.3 and 1 M HFor, pH 1.9) and some basic  
338 eluents (i.e. a mixture of 200 mM NH<sub>3</sub> and 200 mM glycine, pH 9.5) gave very  
339 irreproducible results, or did not elute the protein (i.e. 30 mM NH<sub>4</sub>HCO<sub>3</sub>, pH 7.8 and 1  
340 M NH<sub>3</sub>, pH 11.6). Addition of 20% (v/v) ACN or MeOH to the 30 mM (NH<sub>4</sub>)H<sub>2</sub>PO<sub>4</sub>,  
341 pH 9.0 solution was neither satisfactory, and TTR peak decreased. Overall, the results  
342 showed that elution was mediated by the basic pH, but also by the presence of

343 phosphate anions, which may help to displace the protein from the AuNP surface.  
344 Figure 3B further shows that the maximum amount of TTR was eluted when the plug of  
345 optimized eluent was injected 20 s at 50 mbar.

346 Under the optimized conditions, repeatability was similar to CE-MS studies,  
347 with %RSDs ( $n=3$ ,  $10 \mu\text{g}\cdot\text{mL}^{-1}$  of TTR) of 3.6 and 11.4% for migration time and peak  
348 area, respectively. The microcartridges could be reused until 10 analyses without  
349 significant changes on this performance. Fig. S2 shows a plot of peak area of the  
350 detected TTR after 10 repeated analysis of a  $10 \mu\text{g}\cdot\text{mL}^{-1}$  TTR standard. The  
351 microcartridge was discarded when the peak area of TTR in the EIE decreased more  
352 than 25% compared to the mean value of the first three analyses. Reproducibility  
353 between microcartridges was acceptable, TTR migration times were very similar but  
354 differences on peak areas of the detected TTR until 20% could be observed. The method  
355 was linear ( $r^2>0.998$ ) between 5 and  $25 \mu\text{g}\cdot\text{mL}^{-1}$  (Figure 3C) and the LOD was slightly  
356 lower than  $5 \mu\text{g}\cdot\text{mL}^{-1}$ . This LOD was 50 times lower compared to CE-MS, hence the  
357 sensitivity enhancement was similar compared to IA-SPE-CE-MS using microcartridges  
358 with intact antibodies against TTR [30].

359 Before the analysis of serum samples, the SPE-CE-MS method optimized with  
360 the conventional IT mass spectrometer was transferred to an accurate mass high-  
361 resolution TOF mass spectrometer, which allowed resolving molecular ions from the  
362 different MO TTR proteoforms [28–30]. Figures 4A and 4B show a comparison  
363 between the EIEs and mass spectra obtained for the SPE-CE-MS analysis of a  $10$   
364  $\mu\text{g}\cdot\text{mL}^{-1}$  standard solution of TTR with the IT and TOF mass spectrometers,  
365 respectively. In addition to the slight differences on TTR migration times and peak  
366 shapes in the EIEs due to the particularities of the instrumental set-ups (Figures 4A and  
367 4B i)), the TOF mass spectrometer was able to scan with higher sensitivity, mass

368 accuracy and resolution in a wider  $m/z$  range (Figure 4B ii)). As a result, the inset in  
369 Figure 4B ii) shows that five proteoforms of the MO TTR could be detected in the  
370 deconvoluted mass spectrum. The proteoforms corresponded to TTR-Cys ( $M_{r \text{ theo}} =$   
371 13,880.4022), phosphorylated or sulfonated TTR (TTR-Phosphorylated,  $M_{r \text{ theo}} =$   
372 13,841.2439 or TTR-Sulfonated,  $M_{r \text{ theo}} = 13,841.3283$ , respectively, mass accuracy was  
373 not enough to differentiate this small mass difference [28–30]), dehydroxylated or  
374 conjugated cysteine sulfinic acid TTR (TTR-Dehydroxylated or TTR-Sulfinic,  $M_{r \text{ theo}} =$   
375 13,793.2628, MS/MS would be necessary to differentiate between these isobaric  
376 proteoforms [28–30]), free TTR (Free-TTR,  $M_{r \text{ theo}} = 13,761.2640$ ), and the isoform  
377 resulting from the single amino acid substitution of a cysteine by a glycine at position  
378 10 (TTR-(10) C-G,  $M_{r \text{ theo}} = 13,715.1713$  Da). The LOD for these 5 proteoforms was  
379 around  $1 \mu\text{g}\cdot\text{mL}^{-1}$ , similar to the value obtained with the same TOF mass spectrometer  
380 by IA-SPE-CE-MS in our previous work [30].

381 For the analysis of TTR in serum samples, the off-line sample pretreatment  
382 based on precipitation of the most abundant proteins with 5% (v/v) of phenol that we  
383 applied in a previous work before IA-SPE-CE-MS was investigated [30]. However,  
384 TTR was not detected, current was unstable, and reproducibility was low. This was  
385 probably due to retention of other proteins with similar pI to TTR that remained in the  
386 extract after sample clean-up. Results were also unsatisfactory when phenol  
387 precipitation was repeated twice, or when changes in the amount of salt or phenol were  
388 made. More selective clean-up methods (e.g. immunoprecipitation) were not  
389 investigated to avoid unnecessarily complicating the sample pretreatment. It may  
390 therefore be concluded that the limited selectivity of the AuNPs was especially critical  
391 at the microscale and precluded the analysis of TTR in serum samples when off-line  
392 sample pretreatment was kept simple.

393

#### 394 **4. Conclusions**

395           The study proves that polymeric AuNP@monolith materials can be used to  
396 prepare “plug-and-play” microcartridges for SPE-CE-MS with enough active surface  
397 area to achieve appropriate recoveries and preconcentration factors for protein  
398 biomarkers. Despite the particular benefits of incorporating AuNPs into polymer  
399 monoliths, the selectivity of the hybrid material, which is based on the protein pI, is  
400 compromised when complex biological matrices are analyzed. This investigation could  
401 be regarded as a starting point to design in the future AuNP@monoliths with AuNPs  
402 further modified with more selective ligands (i.e. antibodies, antibody fragments or  
403 aptamers) to find applicability as affinity-based sorbents in the targeted analysis of  
404 peptide and protein biomarkers in biological samples by SPE-CE-MS. Otherwise,  
405 AuNP@monolith-SPE-CE-MS could be also explored to analyze other type of small  
406 molecules (e.g. amino- or thiol-containing compounds) in samples with a lower protein  
407 content or, in general, with a less complex matrix (e.g. pharmaceutical products, drugs  
408 in urine samples or contaminants in environmental water samples).

409

#### 410 **Acknowledgements**

411           This study was supported by the Spanish Ministry of Economy and  
412 Competitiveness (RTI2018-097411-B-I00 and RTI2018-095536-B-I00) and the  
413 Cathedra UB Rector Francisco Buscarons Úbeda (Forensic Chemistry and Chemical  
414 Engineering). Leonardo G. Gagliardi acknowledges the Vice-rectorate for Research of  
415 the University of Valencia for a visiting researcher fellowship (*Atracción de Talento*  
416 program).

417

418 The authors declare no conflicts of interest.

419

## 420 **Figure legends**

421 **Figure 1.** CE-IT-MS for a  $500 \mu\text{g}\cdot\text{mL}^{-1}$  TTR standard. **(A)** Total ion electropherogram  
422 (TIE) and **(B)** mass spectrum with i) 1 M HAc pH 2.3 (acidic BGE) and ii) 10 mM  
423  $\text{NH}_4\text{Ac}$  pH 5.0 (pI BGE). (With the pI BGE a pressure of 100 mbar is applied during the  
424 separation).

425

426 **Figure 2.** Total ion electropherogram (TIE) by AuNP@monolith-SPE-CE-IT-MS for a  
427  $20 \mu\text{g}\cdot\text{mL}^{-1}$  TTR standard with a 10 mM  $\text{NH}_4\text{Ac}$  BGE at pH **(A)** 4.2, **(B)** 5.0 and **(C)**  
428 5.8. (In all cases a pressure of 100 mbar is applied during the separation).

429

430 **Figure 3.** Plot of peak area of the detected TTR vs **(A)** sample loading time at 930  
431 mbar ( $20 \mu\text{g}\cdot\text{mL}^{-1}$  TTR standard, elution 20 s at 50 mbar), **(B)** elution time at 50 mbar  
432 ( $20 \mu\text{g}\cdot\text{mL}^{-1}$  TTR standard, loading 5 min at 930 mbar) and **(C)** concentration of the  
433 loaded TTR standard solution (using the optimized loading and elution times indicated  
434 in **(A)** and **(B)** with an asterisk. Regression parameters in the linear range are shown). In  
435 all AuNP@monolith-SPE-CE-IT-MS experiments, 10 mM  $\text{NH}_4\text{Ac}$  pH 5.0 (pI BGE) is  
436 used for the loading, washing and separation and 30 mM  $(\text{NH}_4)\text{H}_2\text{PO}_4$ , pH 9.0 for the  
437 elution . A pressure of 100 mbar is applied during the separation.

438

439 **Figure 4.** i) Extracted ion electropherogram (EIE) and ii) mass spectrum for a 10  
440  $\mu\text{g}\cdot\text{mL}^{-1}$  TTR standard by **(A)** AuNP@monolith-SPE-CE-IT-MS and **(B)**  
441 AuNP@monolith-SPE-CE-TOF-MS under the optimized conditions. The deconvoluted  
442 mass spectrum is shown for the TOF mass spectrum.

443

444 **References**

- 445 [1] M.C. Breadmore, W. Grochocki, U. Kalsoom, M.N. Alves, S.C. Phung, M.T.  
446 Rokh, J.M. Cabot, A. Ghiasvand, F. Li, A.I. Shallan, A.S.A. Keyon, A.A.  
447 Alhusban, H.H. See, A. Wuethrich, M. Dawod, J.P. Quirino, Recent advances in  
448 enhancing the sensitivity of electrophoresis and electrochromatography in  
449 capillaries in microchips (2016–2018), *Electrophoresis*. 40 (2019) 17–39.  
450 doi:10.1002/elps.201800384.
- 451 [2] A. Šlampová, Z. Malá, P. Gebauer, Recent progress of sample stacking in  
452 capillary electrophoresis (2016–2018), *Electrophoresis*. 40 (2019) 40–54.  
453 doi:10.1002/elps.201800261.
- 454 [3] Z. Malá, P. Gebauer, Recent progress in analytical capillary isotachopheresis,  
455 *Electrophoresis*. 40 (2019) 55–64. doi:10.1002/elps.201800239.
- 456 [4] N.A. Guzman, D.E. Guzman, An emerging micro-scale immuno-analytical  
457 diagnostic tool to see the unseen. Holding promise for precision medicine and P4  
458 medicine, *J. Chromatogr. B Anal. Technol. Biomed. Life Sci.* 1021 (2016) 14–  
459 29. doi:10.1016/j.jchromb.2015.11.026.
- 460 [5] R. Ramautar, G.W. Somsen, G.J. de Jong, Developments in coupled solid-phase  
461 extraction-capillary electrophoresis 2013-2015, *Electrophoresis*. 37 (2016) 35–  
462 44. doi:10.1002/elps.201500401.
- 463 [6] L. Pont, R. Pero-Gascon, E. Gimenez, V. Sanz-Nebot, F. Benavente, A critical  
464 retrospective and prospective review of designs and materials in in-line solid-  
465 phase extraction capillary electrophoresis, *Anal. Chim. Acta.* 1079 (2019) 1–19.  
466 doi:10.1016/j.aca.2019.05.022.
- 467 [7] F. Benavente, S. Medina-Casanellas, E. Giménez, V. Sanz-Nebot, On-line solid-  
468 phase extraction capillary electrophoresis mass spectrometry for preconcentration

- 469 and clean-up of peptides and proteins, in: N.T. Tran, M. Taverna (Eds.), *Capill.*  
470 *Electrophor. Proteins Pept. Methods Protoc. Methods Mol. Biol.*, Springer  
471 Science+Business Media, New York, NY, 2016: pp. 67–84. doi:10.1007/978-1-  
472 4939-4014-1\_6.
- 473 [8] N.E. Baryla, N.P. Toltl, On-line preconcentration in capillary electrophoresis  
474 using monolithic methacrylate polymers, *Analyst*. 128 (2003) 1009–1012.  
475 doi:10.1039/b303701k.
- 476 [9] J.R.E. Thabano, M.C. Breadmore, J.P. Hutchinson, C. Johns, P.R. Haddad,  
477 Capillary electrophoresis of neurotransmitters using in-line solid-phase extraction  
478 and preconcentration using a methacrylate-based weak cation-exchange  
479 monolithic stationary phase and a pH step gradient, *J. Chromatogr. A*. 1175  
480 (2007) 117–126. doi:10.1016/j.chroma.2007.09.069.
- 481 [10] J.R.E. Thabano, M.C. Breadmore, J.P. Hutchinson, C. Johns, P.R. Haddad,  
482 Selective extraction and elution of weak bases by in-line solid-phase extraction  
483 capillary electrophoresis using a pH step gradient and a weak cation-exchange  
484 monolith, *Analyst*. 133 (2008) 1380–1387. doi:10.1039/b804805c.
- 485 [11] J.R.E. Thabano, M.C. Breadmore, J.P. Hutchinson, C. Johns, P.R. Haddad, Silica  
486 nanoparticle-templated methacrylic acid monoliths for in-line solid-phase  
487 extraction-capillary electrophoresis of basic analytes, *J. Chromatogr. A*. 1216  
488 (2009) 4933–4940. doi:10.1016/j.chroma.2009.04.012.
- 489 [12] A. Marechal, F. Jarroson, J. Randon, V. Dugas, C. Demesmay, In-line coupling  
490 of an aptamer based miniaturized monolithic affinity preconcentration unit with  
491 capillary electrophoresis and laser induced fluorescence detection, *J. Chromatogr.*  
492 *A*. 1406 (2015) 109–117. doi:10.1016/j.chroma.2015.05.073.
- 493 [13] J.P. Hutchinson, P. Zakaria, A.R. Bowie, M. Macka, N. Avdalovic, P.R. Haddad,

494 Latex-coated polymeric monolithic ion-exchange stationary phases. 1. Anion-  
495 exchange capillary electrochromatography and in-line sample preconcentration in  
496 capillary electrophoresis, *Anal. Chem.* 77 (2005) 407–416.  
497 doi:10.1021/ac048748d.

498 [14] J.P. Hutchinson, M. MacKa, N. Avdalovic, P.R. Haddad, On-line  
499 preconcentration of organic anions in capillary electrophoresis by solid-phase  
500 extraction using latex-coated monolithic stationary phases, *J. Chromatogr. A.*  
501 1106 (2006) 43–51. doi:10.1016/j.chroma.2005.08.032.

502 [15] Z. Zhang, X. Yan, L. Sun, G. Zhu, N.J. Dovichi, A detachable strong cation  
503 exchange monolith, integrated with capillary zone electrophoresis and coupled  
504 with pH gradient elution, produces improved sensitivity and numbers of peptide  
505 identifications during bottom-up analysis of complex proteomes, *Anal. Chem.* 87  
506 (2015) 4572–4577. doi:10.1021/acs.analchem.5b00789.

507 [16] Z. Zhang, L. Sun, G. Zhu, X. Yan, N.J. Dovichi, Integrated strong cation-  
508 exchange hybrid monolith coupled with capillary zone electrophoresis and  
509 simultaneous dynamic pH junction for large-volume proteomic analysis by mass  
510 spectrometry, *Talanta*. 138 (2015) 117–122. doi:10.1016/j.talanta.2015.01.040.

511 [17] E. Ortiz-Villanueva, F. Benavente, E. Giménez, F. Yilmaz, V. Sanz-Nebot,  
512 Preparation and evaluation of open tubular C18-silica monolithic microcartridges  
513 for preconcentration of peptides by on-line solid phase extraction capillary  
514 electrophoresis, *Anal. Chim. Acta.* 846 (2014) 51–59.  
515 doi:10.1016/j.aca.2014.06.046.

516 [18] Y. Xu, Q. Cao, F. Svec, J.M.J. Fréchet, Porous polymer monolithic column with  
517 surface-bound gold nanoparticles for the capture and separation of cysteine-  
518 containing peptides, *Anal. Chem.* 82 (2010) 3352–3358.

- 519 doi:10.1016/j.jacc.2007.01.076.White.
- 520 [19] Q. Cao, Y. Xu, F. Liu, F. Svec, J.M.J. Fréchet, Polymer monoliths with  
521 exchangeable chemistries : use of gold nanoparticles as intermediate ligands for  
522 capillary columns with varying surface functionalities, *Anal. Chem.* 82 (2010)  
523 7416–7421. doi:10.1021/ac1015613.
- 524 [20] Y. Lv, F. Maya-Alejandro, J.M.J. Fréchet, F. Svec, Preparation of porous  
525 polymer monoliths featuring enhanced surface coverage with gold nanoparticles,  
526 *J. Chromatogr. A.* 1261 (2012) 121–128. doi:10.1016/j.chroma.2012.04.007.
- 527 [21] S. Currivan, D. Connolly, B. Paull, Production of polymer monolithic capillary  
528 columns with integrated gold nano-particle modified segments for on-capillary  
529 extraction, *Microchem. J.* 111 (2013) 32–39. doi:10.1016/j.microc.2012.08.007.
- 530 [22] M. Vergara-Barberán, M.J. Lerma-García, E.F. Simó-Alfonso, J.M. Herrero-  
531 Martínez, Solid-phase extraction based on ground methacrylate monolith  
532 modified with gold nanoparticles for isolation of proteins, *Anal. Chim. Acta.* 917  
533 (2016) 37–43. doi:10.1016/j.aca.2016.02.043.
- 534 [23] M. Catalá-Icardo, C. Gómez-Benito, E.F. Simó-Alfonso, J.M. Herrero-Martínez,  
535 Determination of azoxystrobin and chlorothalonil using a methacrylate-based  
536 polymer modified with gold nanoparticles as solid-phase extraction sorbent,  
537 *Anal. Bioanal. Chem.* 409 (2017) 243–250. doi:10.1007/s00216-016-9993-y.
- 538 [24] H. Alwael, D. Connolly, P. Clarke, R. Thompson, B. Twamley, B. O’Connor, B.  
539 Paull, Pipette-tip selective extraction of glycoproteins with lectin modified gold  
540 nano-particles on a polymer monolithic phase, *Analyst.* 136 (2011) 2619.  
541 doi:10.1039/c1an15137a.
- 542 [25] A. Zhang, F. Ye, J. Lu, S. Zhao, Screening  $\alpha$ -glucosidase inhibitor from natural  
543 products by capillary electrophoresis with immobilised enzyme onto polymer

- 544 monolith modified by gold nanoparticles, *Food Chem.* 141 (2013) 1854–1859.  
545 doi:10.1016/j.foodchem.2013.04.100.
- 546 [26] Y. Liang, C. Wu, Q. Zhao, Q. Wu, B. Jiang, Y. Weng, Z. Liang, L. Zhang, Y.  
547 Zhang, Gold nanoparticles immobilized hydrophilic monoliths with variable  
548 functional modification for highly selective enrichment and on-line  
549 deglycosylation of glycopeptides, *Anal. Chim. Acta.* 900 (2015) 83–89.  
550 doi:10.1016/j.aca.2015.10.024.
- 551 [27] Y. Chen, N. Deng, C. Wu, Y. Liang, B. Jiang, K. Yang, Z. Liang, L. Zhang, Y.  
552 Zhang, Aptamer functionalized hydrophilic polymer monolith with gold  
553 nanoparticles modification for the sensitive detection of human  $\alpha$ -thrombin,  
554 *Talanta.* 154 (2016) 555–559. doi:10.1016/j.talanta.2016.02.054.
- 555 [28] L. Pont, F. Benavente, J. Barbosa, V. Sanz-Nebot, Analysis of transthyretin in  
556 human serum by capillary zone electrophoresis electrospray ionization time-of-  
557 flight mass spectrometry. Application to familial amyloidotic polyneuropathy  
558 type I, *Electrophoresis.* 36 (2015) 1265–1273. doi:10.1002/elps.201400590.
- 559 [29] L. Pont, K. Poturcu, F. Benavente, J. Barbosa, V. Sanz-Nebot, Comparison of  
560 capillary electrophoresis and capillary liquid chromatography coupled to mass  
561 spectrometry for the analysis of transthyretin in human serum, *J. Chromatogr. A.*  
562 1444 (2016) 145–153. doi:10.1016/j.chroma.2016.03.052.
- 563 [30] R. Peró-Gascón, L. Pont, F. Benavente, J. Barbosa, V. Sanz-Nebot, Analysis of  
564 serum transthyretin by on-line immunoaffinity solid-phase extraction capillary  
565 electrophoresis mass spectrometry using magnetic beads, *Electrophoresis.* 37  
566 (2016) 1220–1231.
- 567 [31] E. Giménez, F. Benavente, J. Barbosa, V. Sanz-Nebot, Analysis of intact  
568 erythropoietin and novel erythropoiesis-stimulating protein by capillary

569 electrophoresis-electrospray-ion trap mass spectrometry., *Electrophoresis*. 29  
570 (2008) 2161–2170. doi:10.1002/elps.200700788.

571 [32] H.H. Lauer, G.P. Rozing, eds., *High Performance Capillary Electrophoresis*, 2nd  
572 ed., Agilent Technologies, Waldbronn, Germany, 2014.  
573 doi:10.1371/journal.pone.0016148.

574 [33] E.C. Peters, M. Petro, F. Svec, J.M.J. Fréchet, Molded Rigid Polymer Monoliths  
575 as Separation Media for Capillary Electrochromatography. 1. Fine Control of  
576 Porous Properties and Surface Chemistry, *Anal. Chem.* 70 (1998) 2288–2295.  
577 doi:10.1021/ac9713518.

578 [34] S.H. Brewer, W.R. Glomm, M.C. Johnson, M.K. Knag, S. Franzen, Probing BSA  
579 binding to citrate-coated gold nanoparticles and surfaces, *Langmuir*. 21 (2005)  
580 9303–9307. doi:10.1021/la050588t.

581 [35] W.R. Glomm, Ø. Halskau, A.M.D. Hanneseth, S. Volden, Adsorption behavior  
582 of acidic and basic proteins onto citrate-coated Au surfaces correlated to their  
583 native fold, stability, and pI, *J. Phys. Chem. B*. 111 (2007) 14329–14345.  
584 doi:10.1021/jp074839d.

585 [36] L. Calzolari, F. Franchini, D. Gilliland, F. Rossi, Protein-nanoparticle interaction:  
586 Identification of the ubiquitin-gold nanoparticle interaction site, *Nano Lett.* 10  
587 (2010) 3101–3105. doi:10.1021/nl101746v.

588 [37] L. Ortiz-Martin, F. Benavente, S. Medina-Casanellas, E. Giménez, V. Sanz-  
589 Nebot, Study of immobilized metal affinity chromatography sorbents for the  
590 analysis of peptides by on-line solid-phase extraction capillary electrophoresis-  
591 mass spectrometry, *Electrophoresis*. 36 (2015) 962–970.  
592 doi:10.1002/elps.201400374.

593

The authors declare no conflicts of interest.

## **CRedit authorship contribution statement**

**Laura Pont:** Methodology, Validation, Investigation, Writing original draft, Writing – review & editing. **Gemma Marin:** Methodology, Validation, Investigation, Writing – review & editing. **María Vergara-Barberán:** Methodology, Validation, Investigation, Writing – review & editing. **Leonardo G. Gagliardi:** Conceptualization, Writing – review & editing. **Victoria Sanz-Nebot:** Conceptualization, Writing – review & editing, Supervision, Funding acquisition. **José M. Herrero-Martínez:** Conceptualization, Writing – review & editing, Supervision, Project administration, Funding acquisition, **Fernando Benavente:** Conceptualization, Writing original draft, Writing – review & editing, Supervision, Project administration, Funding acquisition.

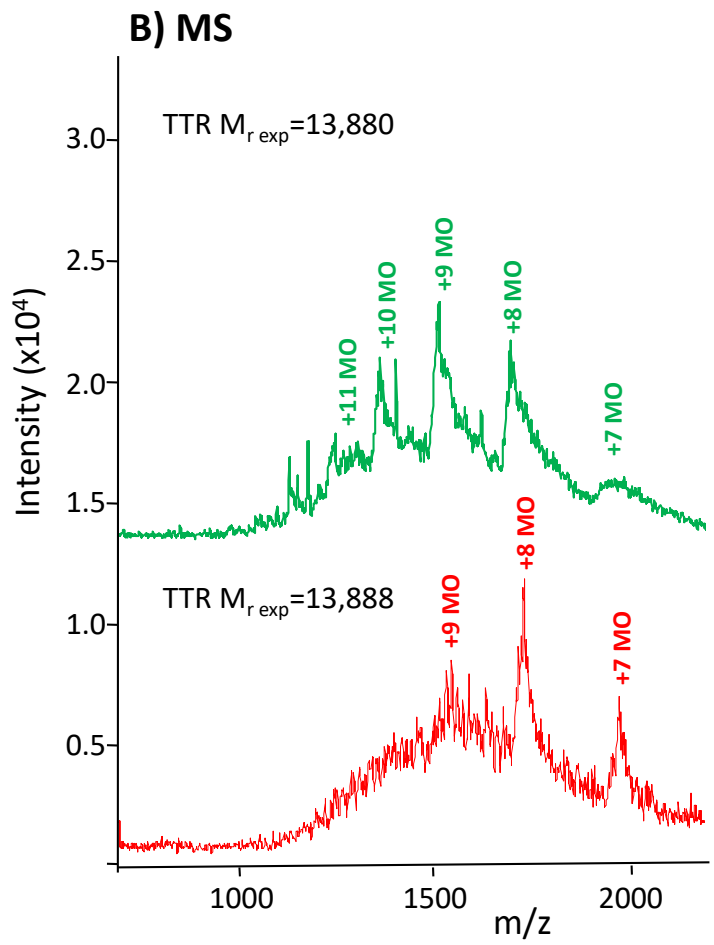
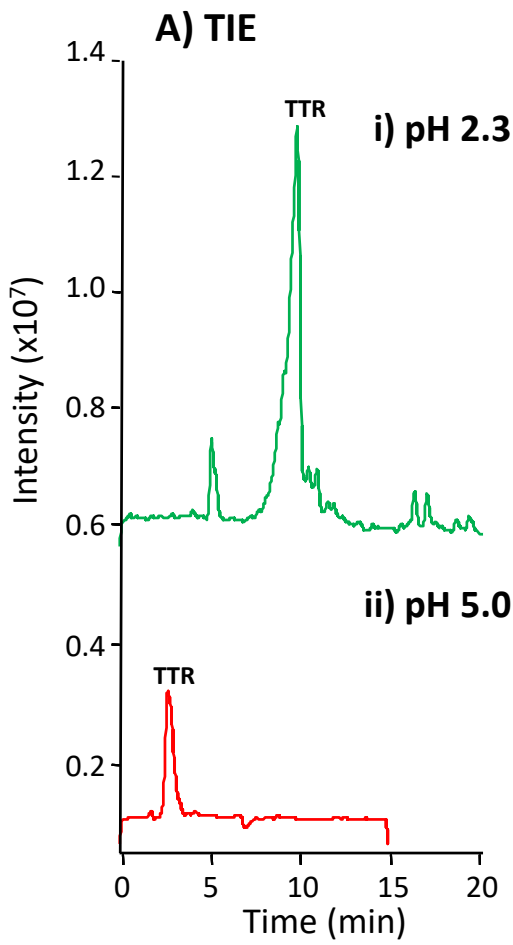


**Figure 1**

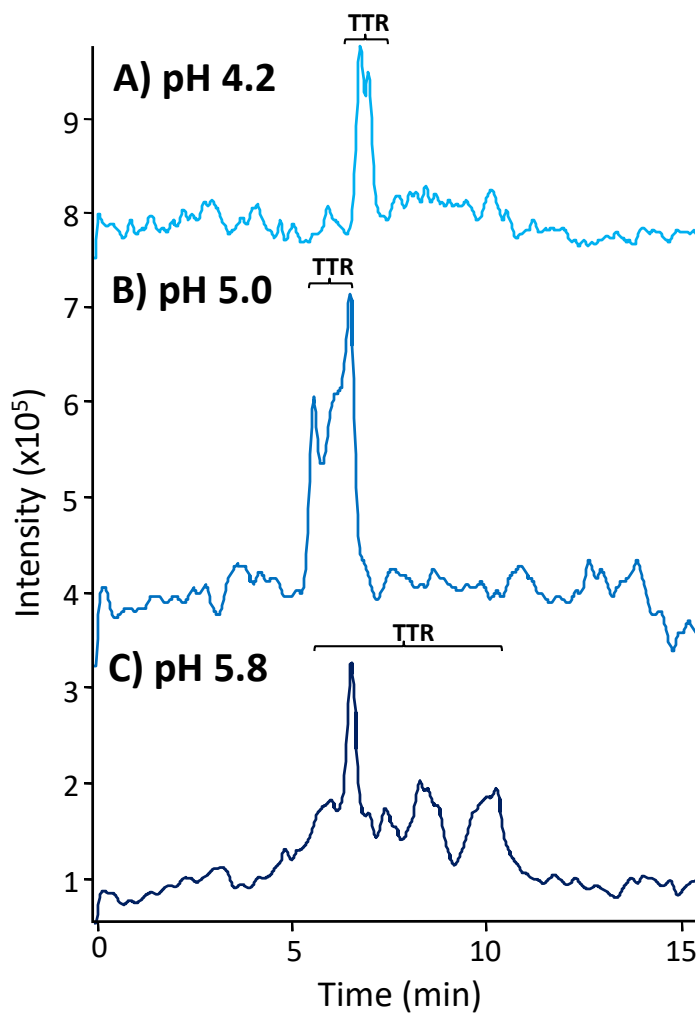
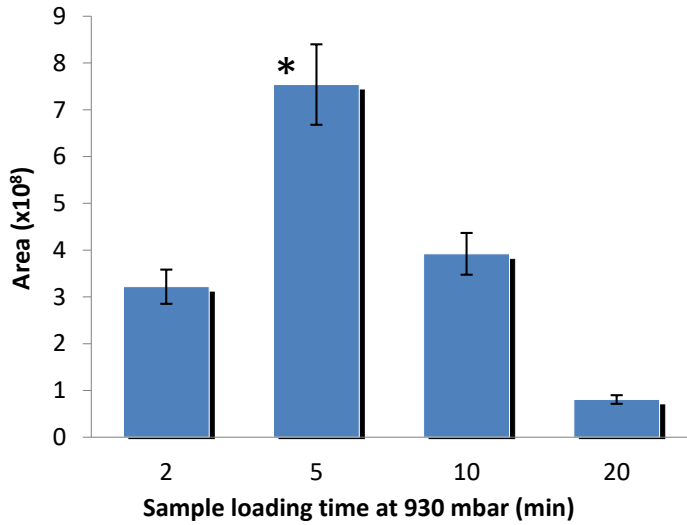
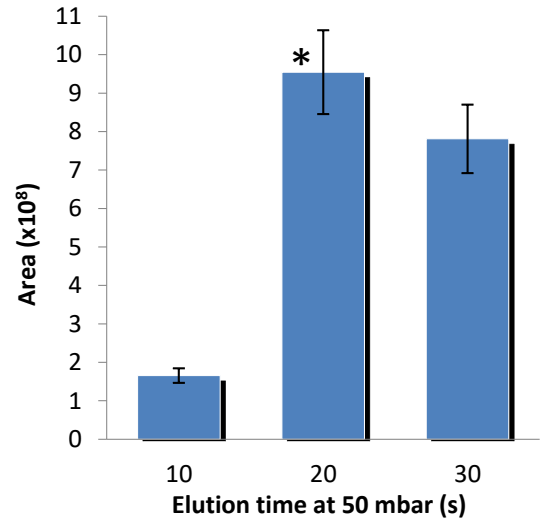


Figure 2

### A) Sample loading



### B) Eluent volume



### C) Linearity

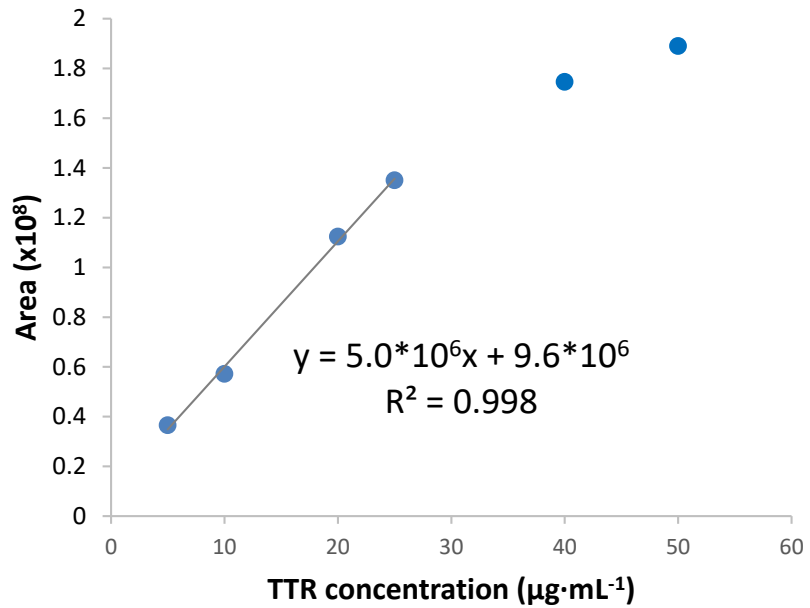
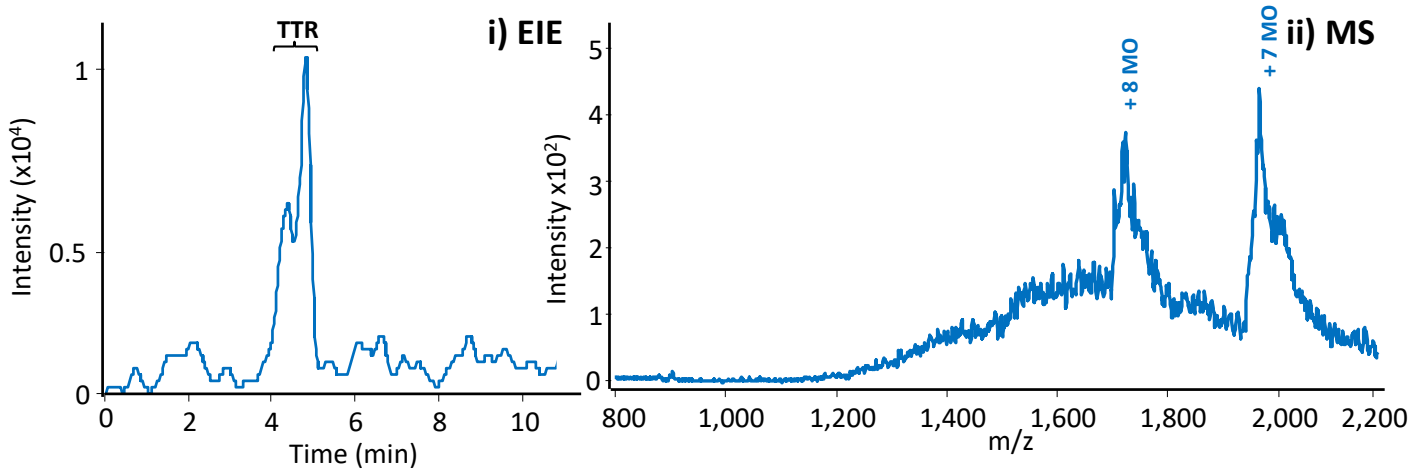


Figure 3

### A) AuNP@monolith-SPE-CE-IT-MS



### B) AuNP@monolith-SPE-CE-TOF-MS

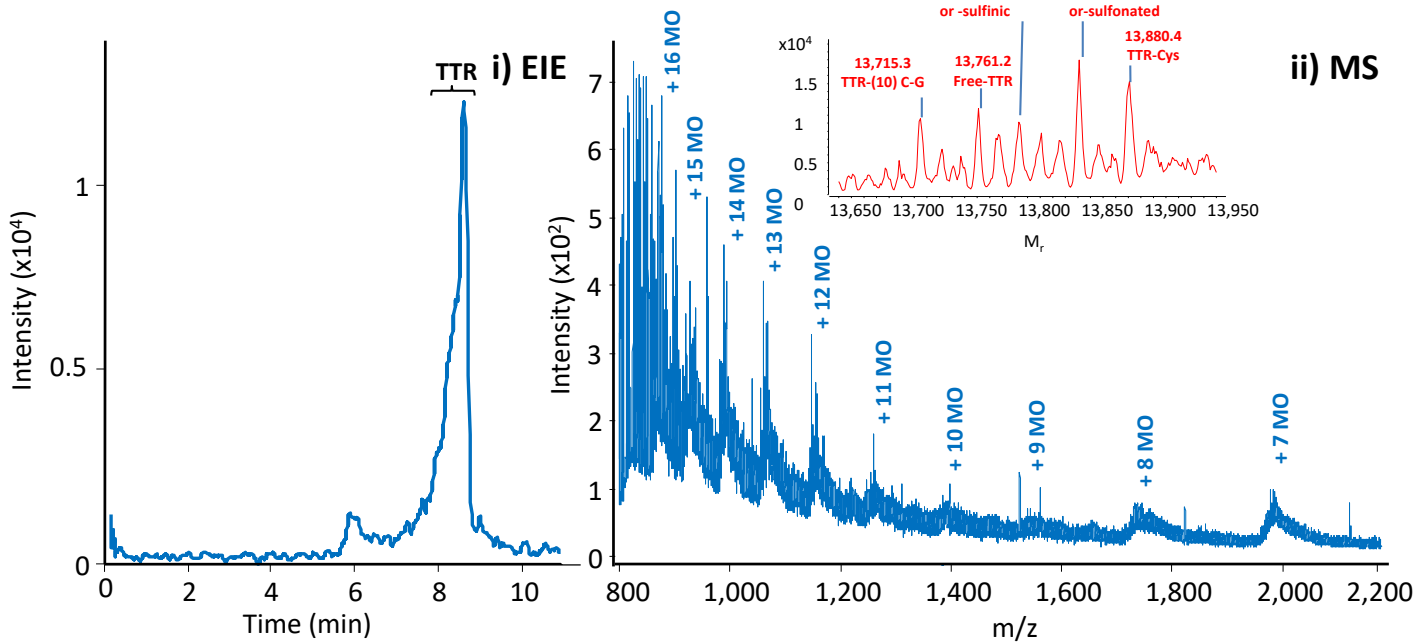


Figure 4

## SUPPLEMENTARY MATERIAL

### **Polymeric monolithic microcartridges with gold nanoparticles for the analysis of protein biomarkers by on-line solid-phase extraction capillary electrophoresis-mass spectrometry**

Laura Pont<sup>1</sup>, Gemma Marin<sup>1</sup>, María Vergara-Barberán<sup>2</sup>, Leonardo G. Gagliardi<sup>3</sup>,  
Victoria Sanz-Nebot<sup>1</sup>, José M. Herrero-Martínez\*<sup>2</sup>, Fernando Benavente\*<sup>1</sup>

<sup>1</sup>Department of Chemical Engineering and Analytical Chemistry, Institute for Research on Nutrition and Food Safety (INSA·UB), University of Barcelona, C/Martí i Franquès 1-11, 08028 Barcelona, Spain

<sup>2</sup>Department of Analytical Chemistry, University of Valencia, C/Doctor Moliner 50, 46100 Burjassot, Spain

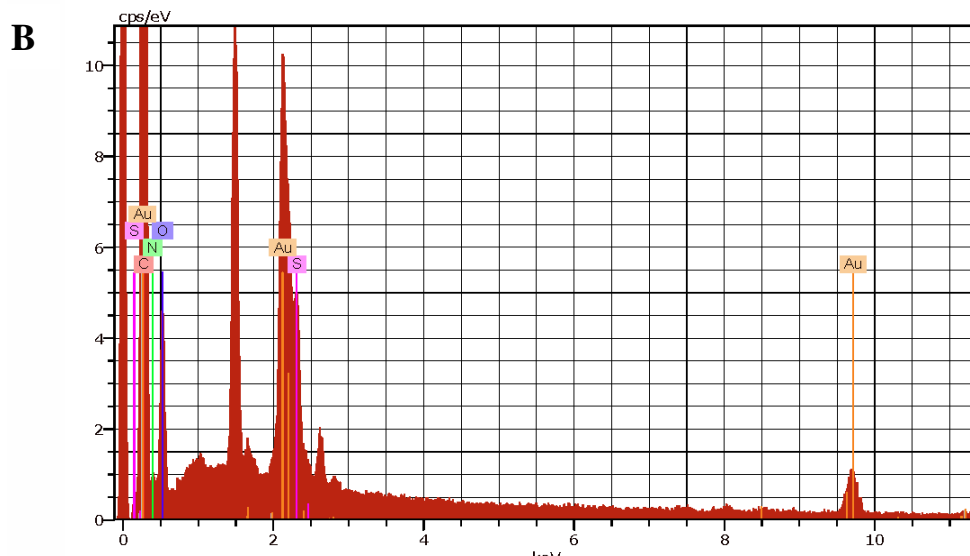
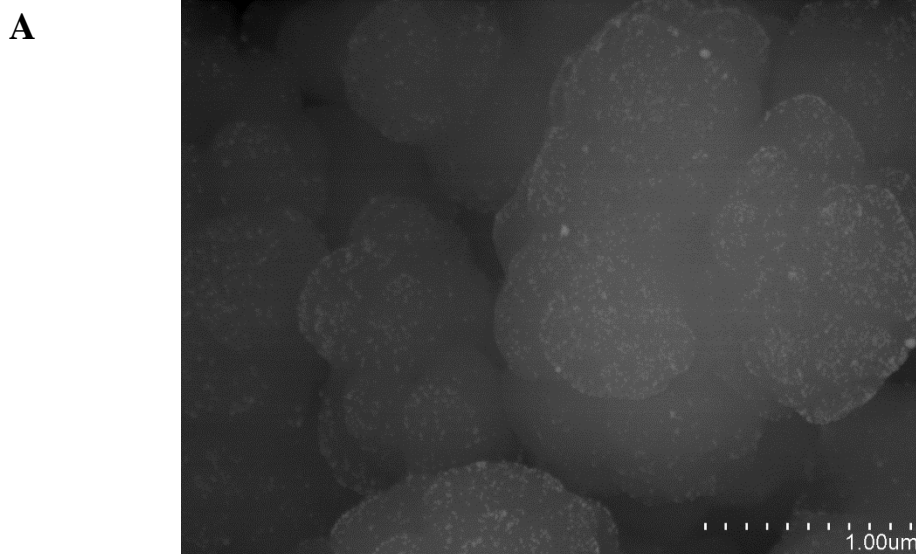
<sup>3</sup>Laboratorio de Investigación y Desarrollo de Métodos Analíticos, LIDMA, Facultad de Ciencias Exactas, Universidad Nacional de La Plata, CIC-PBA CONICET, C/ 47 esq. 115, B1900AJL La Plata, Argentina

\*Corresponding authors: fbenavente@ub.edu (F. Benavente, PhD)

Tel: (+34) 934039116, Fax: (+34) 934021233

and jmherrer@uv.es (J. M. Herrero-Martínez, PhD)

Tel: (+34) 963544062, Fax: (+34) 963544436



Spectrum: 1

Element	Series	unn. C [wt.%]	norm. C [wt.%]	Atom. C [at.%]	Error [wt.%]
Carbon	K-series	80.27	66.56	81.34	9.1
Nitrogen	K-series	7.69	6.37	6.68	1.5
Oxygen	K-series	13.34	11.06	10.15	2.0
Sulfur	K-series	2.01	1.67	0.76	0.1
Gold	L-series	17.30	14.35	1.07	0.6
Total:		120.61	100.00	100.00	

**Figure S1.** (A) SEM micrograph (at 35,000 × magnification) and (B) EDAX data collected in a 1 μm<sup>2</sup> area of of the polymer AuNP@monolith.

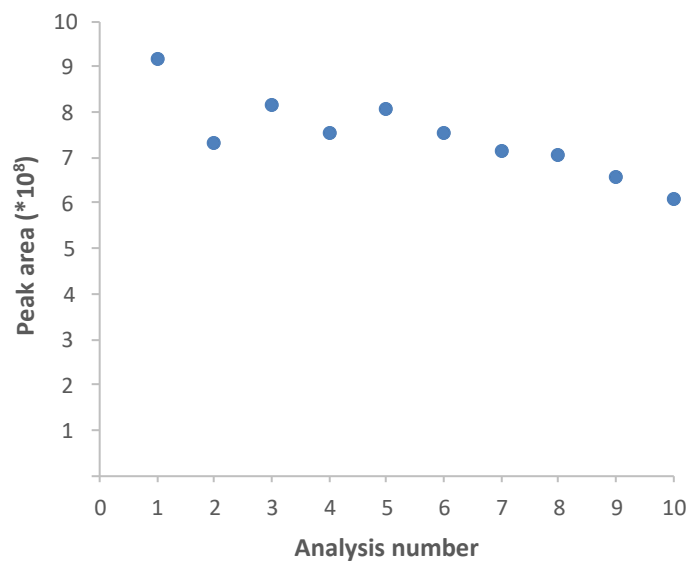


**Figure S2.** Plot of peak area of the detected TTR after repeated analysis of a  $10 \mu\text{g}\cdot\text{mL}^{-1}$  TTR standard under the optimized conditions by AuNP@monolith-SPE-CE-IT-MS. The microcartridge was discarded when the peak area of TTR in the EIE decreased more than 25% compared to the mean value of the first three analyses with the microcartridge under consideration (analysis number=10).